Eur. Phys. J. Special Topics **224**, 3041–3054 (2015)

DOI: 10.1140/epjst/e2015-02605-6

THE EUROPEAN PHYSICAL JOURNAL SPECIAL TOPICS

Regular Article

Motion and vibration control of a slewing flexible structure by SMA actuators and parameter sensitivity analysis

F.C. Janzen[1,a], A.M. Tusset[2,b], V. Piccirillo[2,c], J.M. Balthazar[3,d], and R.M.L.R.F. Brasil[4,e]

[1] Universidade Estadual Paulista, UNESP, Bauru, SP, Brazil
[2] Federal Technological University of Paraná, UTFPR, Ponta Grossa, PR, Brazil
[3] Technological Institute of Aeronautics, ITA, São Jose dos Campos, SP, Brazil
[4] Federal University of ABC, UFABC, Santo Andre, SP, Brazil

Received 21 August 2015 / Received in final form 9 September 2015
Published online 20 November 2015

Abstract. This work presents two approaches to the problem of vibration and positioning control of a flexible structural beam driven by a DC motor. The position is controlled by the current applied to the DC motor armature. A Shape Memory Alloy (SMA) actuator controls vibrations of the flexible structural beam. The State Dependent Riccati Equation (SDRE) technique is used to provide a control action which uses sub-optimal control and system local stability search. The robustness of these two controllers is tested by sensitivity analysis to parametric uncertainties. Numerical simulations results are presented to demonstrate the effectiveness of the proposed control strategy.

1 Introduction

The use of flexible links in robotic systems and aerospace structures have motivated many recent research works. In some applications, such as space assemblies or robots acting in constrained workspaces, the use of flexible link systems presents some advantages, like cost effective lunching, lower power consumption and lower material consumption, with the consequence of mass and stiffness reduction. The main disadvantage brought by flexibility is larger vibration amplitude leading to accuracy and dexterity decrease. This problem can be solved by applying an active vibration control system (Tokhi and Azad, 2008).

Garcia and Inman (1991) have proposed an active vibration control of a slewing flexible structure by bonding piezoelectric ceramic (PZT), which is considered a smart material, and the flexible structure is controlled by applying voltage variations to

[a] e-mail: fcjanzen@utfpr.edu.br
[b] e-mail: a.m.tusset@gmail.com
[c] e-mail: piccirillo@utfpr.edu.br
[d] e-mail: jmbaltha@gmail.com
[e] e-mail: reyolando.brasil@ufabc.edu.br

the PZT's. This approach presents a voltage peak reduction on the motor and reduction of the maximum tip deflection of the beam.

Some other smart material can be used to actively control vibrations of flexible structures, as shown by Janzen et al. (2014) and Ge et al. (2006). The results presented in those papers demonstrate that the application of another smart material, known as Shape Memory Alloys (SMA), can reduce vibrations due to flexibility and, therefore, result in better performance. Shape memory hybrid composites can present functions such as active modal modification and high damping, which can be utilized to tune the performance of a smart structure (Wei and Sandström, 1998). Yuvaraja and Senthilkumar (2012) present in their work a comparison between SMA and PZT actuators on a composite beams. They conclude that the SMA actuators are more efficient because the lower required actuation voltage.

SMAs have the ability to return to a defined shape or size by applying an adequate thermal load. This is known as Shape Memory effect (SME). This is a consequence of displacements of the crystalline structure of the material between two phases, known as martensite and austenite (Piccirillo et al. 2008). The device can be trained to have a particular shape in the austenite phase. Due to the martensitic transformation, an apparent plastic deformation can be recuperate. When this materials are heated to a certain temperature, large contraction forces are created due to the shape recovery which happens during the martensitic transformation (Sepiani et al., 2009). This phase change effect of the material displays hysteretic characteristics, which need to be considered when applying these materials as vibration actuators (Romano, 2009).

Many control techniques have been applied to SMA deformations, such as linear PID controllers, as shown in (Ikuta, 1990), and non-linear controllers as used by (Elahina et al., 2004). Janzen et al. (2014) show the application of a SDRE (State Dependent Riccati Equation) controller to a slewing flexible beam driven by a DC motor while SMA actuators were used to reduce vibration peak amplitude.

The SDRE control technique is considered a sub optimal control which searches for a local stability of a system (Mracek and Cloutier, 1998). The advantage of this control technique is that it does not cancel possible benefits provided by nonlinearities of the system. This is due to the fact that to apply this technique it is not necessary to linearize the system (Molter, 2010; Fenili and Balthazar, 2011; Tusset et al., 2012a, 2012b, 2013, 2015; Lima et al., 2014; Balthazar et al., 2014).

The main objective of the present work is to model and control a flexible beam structure in a slewing motion driven by a DC motor and actuated upon by a SMA actuator in order to control vibrations peak amplitude. Here, two cases are presented. In the first one, only the angular positioning of the beam like structure is controlled. The second one demonstrates the application of a vibration control applied to the positioning control. The control technique to be applied to both the cases is the SDRE technique. Numerical simulations are performed to present the behavior of the system and controllers. A parametric sensitivity analysis is carried out to show the robustness of the applied control technique.

2 Dynamic equations of the system

2.1 Motor/Beam equation

The dynamical system analyzed here consists of a direct current motor that is the position actuator, and a flexible composite aluminum beam with a NiTi SMA actuator. This composite beam exhibits motions in a slewing trajectory. A schematic representation of the system is presented in Fig. 1.

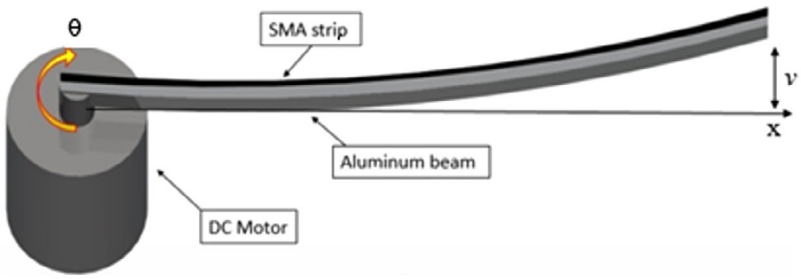

Fig. 1. Schematic of the analyzed system.

In Fig. 1, $\theta(t)$ represents the rigid-body motion, $v(x,t)$ is the elastic deflection of the beam. The total displacement of the beam for small angle rotations is given by Eq. (1) (Ephrahim and Inman, 1990; Tokhi and Azad, 2008).

$$y\left(x,t\right) = x\theta\left(t\right) + v(x,t). \tag{1}$$

In this work large angular displacements and small transversal displacements of the beam are considered as showed in Fenili and Balthazar (2004).

The governing equations of motion are obtained using the extended Hamilton's principle, an energy method described by Gantmacher (1975) and Meirovitch (1967). For this method, the kinetic and potential energy expression need to be written. The kinetic energy of the rotating beam is given by (Fenili et al., 2003).

$$T = \frac{1}{2}p\int_0^L \left(\dot{v} + x\dot{\theta}\right)^2 + (v\dot{\theta})^2 dx \tag{2}$$

where: p is the mass per unit length and L is the initial length of the beam. A dot over the variable symbol denotes time derivative. This work does not consider the hub kinetic energy.

The potential (strain) energy of the beam can by written as:

$$V = \frac{1}{2}\int_0^L EI\left(v''\right)^2 dx \tag{3}$$

where I is the moment of inertia of the cross-section of the beam and E is the Young's modulus of the beam's material. Two dashes to the right of the variable symbol denotes x second derivative.

Introducing the kinetic and potential energies of Eq. (1) and Eq. (2) in the extended Hamilton principle, considering the torque τ as a non-conservative force, and solving, as described in Meirovitch (1967), the following equations of motion are obtained:

$$\int_0^L p\left(\ddot{v}x + x^2\ddot{\theta} + \ddot{\theta}v^2 + 2\dot{\theta}v\dot{v}\right)dx = \tau \tag{4}$$

$$\int_0^L \left[p\left(\ddot{v} + x\ddot{\theta} - \dot{\theta}^2 v\right) EIv^{IV}\right]dx = 0. \tag{5}$$

Next, the assumed modes technique is applied, substituting Eq. (6), as described in Meirovitch (1967), into Eq. (4) and Eq. (5), considering only the first vibration mode of the beam. The beam is modeled as a cantilever Euler Bernoulli beam represented

by Eq. (7), as described in Ephrahim and Inman (1990). The discretized equation of motion of the beam is given by Eq. (8).

$$v(x,t) = \sum_{i=1}^{N} \phi_i(t)\, q_i(t) \tag{6}$$

$$\phi^{IV} - \omega^2 \phi = 0 \tag{7}$$

$$\ddot{q}_1 = -\mu \dot{q}_1 - \omega_1^2 q_1 - \alpha \ddot{\theta} + \dot{\theta}^2 q_1 \tag{8}$$

where: $\alpha = \int_0^L x\phi_1 dx$, the natural frequency of the beam is $\omega_1 = (a_1 L)^2 \sqrt{\frac{EI}{\mu L^4}}$, and the term $\mu \dot{q}_1$, which represents the structural damping, is added applying the assumed mode technique.

Ephrahim and Inman (1990) give the dynamical behavior of beam coupled to the DC motor:

$$\dot{i}_a = -a_1 i_a - a_2 \dot{\theta} \tag{9}$$

$$\ddot{\theta} = -b_1 \dot{\theta} + b_2 i_a + b_3 q_1 \tag{10}$$

$$\ddot{q}_1 = -\mu \dot{q}_1 - \omega_1^2 q_1 - \alpha \ddot{\theta} + \dot{\theta}^2 q_1 \tag{11}$$

where: $a_1 = \frac{R}{L_m}$, $a_2 = \frac{K_b}{L_m}$, $b_1 = \frac{c}{I_{e+I_m}}$, $b_2 = \frac{K_t}{I_{e+I_m}}$, $b_3 = \frac{EI\phi''(0)}{I_{e+I_m}}$. L_m is the motor inductance, R is the armature resistance of the motor, K_b is the constant counter electromotive force of the motor, I_e is the inertia associated with the motor shaft. I_m represents the inertia of internal parts of the motor, c represents the internal friction of motor, K_t is the motor torque constant, q_1 represents the amplitude of the first vibration mode of the beam, θ represents angular displacement, i_a represents the electric current in the motor armature, ϕ is the modal shape and the term $\dot{\theta}^2 q_1$ is the centripetal stiffness.

The term $b_3 q_1$ in Eq. (10) represents the bending moment of the beam acting upon the motor so that the beam dynamic equation and the DC motor equations are now coupled.

2.2 Shape memory alloy dynamics

The SMA constitutive model used in this work is based on the work from Brinson (1993). The purpose of this paper is to study the biased actuator, which is composed of a SMA element and the bending moment of the beam will be used as the bias spring. This SMA actuator is used for vibration control. The SMA element is deformed at low temperature, before being connected to the beam. When it is heated, the recovery force which is generated pulls the beam, thus storing energy in it. When the SMA element is cooled, the energy stored in the beam is released and the SMA element deforms back, thus completing the cycle. We consider that the actuation will occur due to application of an electric current to the SMA which changes its temperature. The stress variation in the SMA is represented by Eq. (12).

$$\dot{\sigma} = D\dot{\varepsilon} + \Omega\dot{\xi} + \Theta\dot{T} \tag{12}$$

where σ is the stress in the SMA, D is the SMA Young modulus, given by Eq. (13), ε is the SMA strain, Ω is the phase transformation contribution factor, represented

by Eq. (14), ξ is the phase transformation factor, Θ is the SMA thermal expansion factor and T is the SMA temperature.

$$D = \xi E_M + (1 - \xi) E_A \tag{13}$$

$$\Omega = D\varepsilon_0. \tag{14}$$

Equation (15) represents the strain variation of the SMA, which can be described as the strain of the beam. To simplify the SMA layer is very thin in relation to the aluminum beam.

$$\dot{\varepsilon} = \frac{(b_3 q_1 z_{sma})}{I E_t} \tag{15}$$

where: $b_3 q_1$ is the bending moment of the beam, z_{sma} is the distance between the center of the beam to the end point of the beam in the z axis, and E_t describes the effective Young modulus of the composite beam, which is calculated with Eq. (16) (Ramos, et al., 2007).

$$E_t = \frac{E^2 \left(\frac{t_f}{t}\right)^4 + D^2 \left(\frac{t_s}{t}\right)^4 + 2ED \left(\frac{t_s}{t}\right) \left(\frac{t_f}{t}\right) \left[2 \left(\frac{t_f}{t}\right)^2 + 2 \left(\frac{t_s}{t}\right)^2 + 3 \left(\frac{t_s}{t}\right) \left(\frac{t_f}{t}\right)\right]}{E \left(\frac{t_f}{t}\right) + D \left(\frac{t_s}{t}\right)} \tag{16}$$

where t_f, t_s and t are the aluminum beam, SMA actuator and total thickness respectively.

Equations (17–18) are the state equations during heating and cooling, respectively.

$$\dot{\xi} = -\frac{\xi_M}{2} \sin[a_A (T - A_s) + bA\sigma][a_A \dot{T} + b_A \dot{\sigma}] \tag{17}$$

$$\dot{\xi} = -\frac{1 - \xi_A}{2} \sin[a_M (T - M_f) + b_M \sigma][a_M \dot{T} + b_M \dot{\sigma}] \tag{18}$$

where: $a_A = \frac{\pi}{A_f - A_s}$, $a_M = \frac{\pi}{M_s - M_f}$, $b_a = \frac{-a_A}{C_A}$, $b_M = \frac{-a_M}{C_M}$ and A_f, is the austenite phase finish and A_s is the austenite phase start and M_s, M_f are the martensitic phase start and finish, respectively. C_A and C_M are curve fitting parameters (Elahinia and Ashrafiuon, 2002).

Equation (19) is the heat transfer function for the SMA which consist of electrical heating and natural convection. The heat transfer between the SMA and the aluminum beam is neglected.

$$\dot{T} = \frac{\frac{v^2}{R} - hA(T - T_{in})}{mcp} \tag{19}$$

where, V is the electric voltage applied to the SMA, R is the SMA electrical resistance, c_p is the specific heat, m is the mass per unit length, h is the heat convection coefficient and T_{in} is the ambient temperature.

2.3 Coupling between the Beam and the SMA

The coupling between the SMA and the aluminum beam can be described through the effective Young modulus of the two components, SMA and aluminum beam

Eq. (16). The new Young modulus E_t can be substituted in the variables b_3 and ω_1 as shown in Eqs. ((20)–(21)).

$$b_3 = \frac{E_t I \phi''(0)}{I_e + I_M} \tag{20}$$

$$\omega_1 = (a_1 L)^2 \sqrt{\frac{E_t I}{\mu L^4}}. \tag{21}$$

The second coupling is given by subtraction of the SMA and beam stresses, which have a direct effect over the bending moment of the beam. The bending moment of the beam can be described as shown in Eq. (22).

$$b_3 q_1 = \frac{\sigma_v I}{z} \tag{22}$$

where: σ_v is the aluminum beam stress. Subtracting the SMA stress from the beam stress, Eq. (22) can be rewritten as shown in Eq. (23), which is the bending moment of the set aluminum beam and SMA.

$$M = b_3 q_1 - \frac{\sigma I}{z_{sma}}. \tag{23}$$

Substituting Eq. (23) into Eq. (10) and Eq. (12) the complete dynamic equations of motion for the system described in this work are given by Eqs. ((24)–(28)).

$$i_a = -a_1 i_a - a_2 \dot{\theta} \tag{24}$$

$$\ddot{\theta} = b_1 \dot{\theta} + b_2 i_a + M \tag{25}$$

$$\ddot{q}_1 = -\mu \dot{q}_1 - {\omega_1}^2 q_1 - \alpha \ddot{\theta} + \dot{\theta}^2 q_1 \tag{26}$$

$$\dot{\sigma} = D(\dot{\varepsilon}) + \Omega(\dot{\xi}) + \Theta(\dot{T}) - \left(\frac{b_3 q_1 z_{sma}}{I} \right) \tag{27}$$

$$\dot{T} = \frac{\frac{v^2}{R} - hA(T - T_{in})}{mcp}. \tag{28}$$

3 Control technique

The control proposed in this paper is formulated to find the control function u that transfers the system of the initial state Eq. (29) to the final state Eq. (30):

$$x\,(0) = x_0 \tag{29}$$

$$x\,(\infty) = x^* \tag{30}$$

where: $x = [x_1 x_2 x_3 x_4 x_5]^T$ and x^* is the desired state.

Equations (9–11) can be parameterized in first order equations and rewritten to the state-dependent coefficient (SDC) (Molter et al., 2010).

$$\dot{x} = A(x)x + Bu. \tag{31}$$

A state feedback is adopted before the feedback output to enhance the performance of the controller. The quadratic cost function for the regulator problem is given by Eq. (32).

$$J = \frac{1}{2}\int_{t_0}^{\infty} \left[y^T Q\left(x\right) y + u^T R\left(x\right) u\right] dt \tag{32}$$

where, $y = [x - x*]$ represents the deviations from the desired trajectory, and $Q\left(x\right)$ is a semi-positive-definite matrix and $R\left(x\right)$ is positive definite. There are weighting matrices on the control inputs and outputs, respectively. In a point wise linear fashion, these matrices are assumed with constant coefficients.

The minimization of the functional Eq. (32) implies the minimization of the system deviation Eq. (31), of the desired state (y=$[x - x*]$), and of the applied feedback control (u).

Assuming full state feedback, the control law is given by Nozaki et al. (2013).

$$u = -R^{-1}\left(x\right) B^T\left(x\right) P\left(x\right) y. \tag{33}$$

The state-dependent Riccati equation to obtain $P\left(x\right)$, is given by:

$$A^T\left(x\right) P\left(x\right) + P\left(x\right) A\left(x\right) - P\left(x\right) B\left(x\right) R^{-1}\left(x\right) B^T\left(x\right) P\left(x\right) + Q\left(x\right) = 0. \tag{34}$$

System (31) is controllable if the rank of the matrix M is n, as follows:

$$M = \left[B \quad A_{n\times n}B \quad \ldots \quad A^n{}_{n\times n}B\right]. \tag{35}$$

3.1 Angular positioning control

In systems like robotic manipulators, the position of the end point of the flexible link, in this work represented by a flexible beam, needs to be controlled. Considering the case in which just the position is controlled, system ((24)–(26)) can be written in the state space form as shown in Eq. (36).

$$\begin{aligned}
\dot{x}_1 &= -a_1 x_1 - a_2 x_3 + d_1 u_1 \\
\dot{x}_2 &= x_3 \\
\dot{x}_3 &= -b_1 x_3 + b_2 x_1 + b_3 x_4 - (\sigma I_{SMA}/z_{SMA}) \\
\dot{x}_4 &= x_5 \\
\dot{x}_5 &= -\mu x_5 - \omega^2 x_4 + \alpha b_1 x_3 - \alpha b_2 x_1 - \alpha b_3 x_4 + x_3^2 x_4
\end{aligned} \tag{36}$$

where $x_1 = i_a$, $x_2 = \theta$, $x_3 = \dot{\theta}$, $x_4 = q$, $x_5 = \dot{q}$, the control signal u_1 is the voltage applied to the DC motor terminals and $d_1 = 1/L_m$. Equation (36) can be rewritten in form of Eq. (31), where:

$$A(x) = \begin{bmatrix} (-a_1 - x_2) & x_1 & -a_2 & 0 & 0 \\ 0 & 0 & 1 & 0 & 0 \\ b_2 & 0 & -b_1 & b_3 & 0 \\ 0 & 0 & 0 & 0 & 1 \\ -\alpha b_2 & 0 & \alpha b_1 & (-\omega_1^2 - \alpha b_3 + x_3^2) & -\mu \end{bmatrix} \text{ and } B = \begin{bmatrix} \frac{1}{L_m} \\ 0 \\ 0 \\ 0 \\ 0 \end{bmatrix}.$$

Table 1. Parameters for numerical simulation.

$c = 4.629\ (10^{-3})$ Nms/rad	$K_t = 0.23309$ Nm/A	E_A =28(10^9)N/m^2	$\varepsilon_{0=}$0,02678
$K_b = 0.23309$ V/rad/s	$L_m = 1.6\ (10^{-3})$ H	M_s =52 °C	$\Theta = -0,055$
$\beta = 1$	$R = 1.5\,\Omega$	M_f =42 °C	C_M =10.3 (10^6)
$I_m = 8.02\ (10^{-5})$kg.m^2	$I_e = 6.540\ (10^{-7})$kg.m^2	A_s =68 °C	C_A =10.3 (10^6)
L =0.5 m	$\mu = 0.19$ Kg/ms	A_f =78 °C	ξ_M =1
E =0.7 (10^{11})N/m^2	$I = 1.1093\ (10^{-12})$ m^4	A =5 (10^{-6})m^2	ξ_A =0
W =7.3584 rad/s	$\phi'' = 0.54182$	T_{in} =20 °C	h =120 W/(m^2°C)
$\alpha = 0.234$	E_M =75 (10^9) N/m^2	$R_{SMA} = 4\Omega$	σ_{in} =75 (10^6)Pa

In general, $A(x)$ is unique only if A(x) is composed only by scalars. Else, it is possible to write them in another state-dependent coefficient parametrization (Banks, Lewis and Tram, 2007). Defining:

$$x^* = \begin{bmatrix} 0 \\ 1 \\ 0 \\ 0 \\ 0 \end{bmatrix}, \quad Q = 10^4 \begin{bmatrix} 1 & 0 & 0 & 0 & 0 \\ 0 & 1 & 0 & 0 & 0 \\ 0 & 0 & 1 & 0 & 0 \\ 0 & 0 & 0 & 1 & 0 \\ 0 & 0 & 0 & 0 & 1 \end{bmatrix} \text{ and } R = [1].$$

where: x^* are the desired states which in this work is a 1 radian displacement of the beam position, and Q and R are the matrices used to calculate the Riccati equation Eq. (34). Q and R are positive definite matrices, which guarantees the optimal solution of the feedback regulator problem performance (Mracek and Cloutier, 1998).

3.2 Positioning and vibration control

Considering now the case in which positioning and vibrations of the beam are controlled, a second SDRE controller is added to the system presented in Sect. 3.1. This controller is responsible to lead vibrations of the beam to zero. Considering Eqs. ((26)–(28)) written in form of Eq. (31) where:

$$A(x) = \begin{bmatrix} x_4 & 1 & (-x_4^2 x_1) \\ (-\omega_1^2 - \alpha b_3 - x_3^2) & (-\mu x_5 T) & -x_5^2 \\ T^2 & 0 & (\frac{-hA}{mc_p} - Tx_1) \end{bmatrix} \text{ and } B = \begin{bmatrix} 0 \\ 0 \\ \frac{1}{R_{SMA} mc_p} \end{bmatrix}$$

where $x_4 = q$ and $x_5 = \dot{q}$.

Defining:

$$\begin{bmatrix} x_4^* \\ x_4^* \\ T^* \end{bmatrix} = \begin{bmatrix} 0 \\ 0 \\ 0 \end{bmatrix}, Q = 100 \begin{bmatrix} 1 & 0 & 0 \\ 0 & 10 & 0 \\ 0 & 0 & 2 \end{bmatrix} \text{ and } R = [10^{-2}].$$

4 Numerical simulations results

Parameters chosen for our numerical simulations are presented in Table 1, obtained from Janzen et al. (2014) and Elahinia and Ashrafiuon (2002).

Figure 2 shows the numerical simulation results for the positioning control of the beam presented in Sect. 3.1. Initial conditions for these simulations are: $x_1 = 0$, $x_2 = 0$, $x_3 = 0$, $x_4 = 0$, $x_5 = 0$.

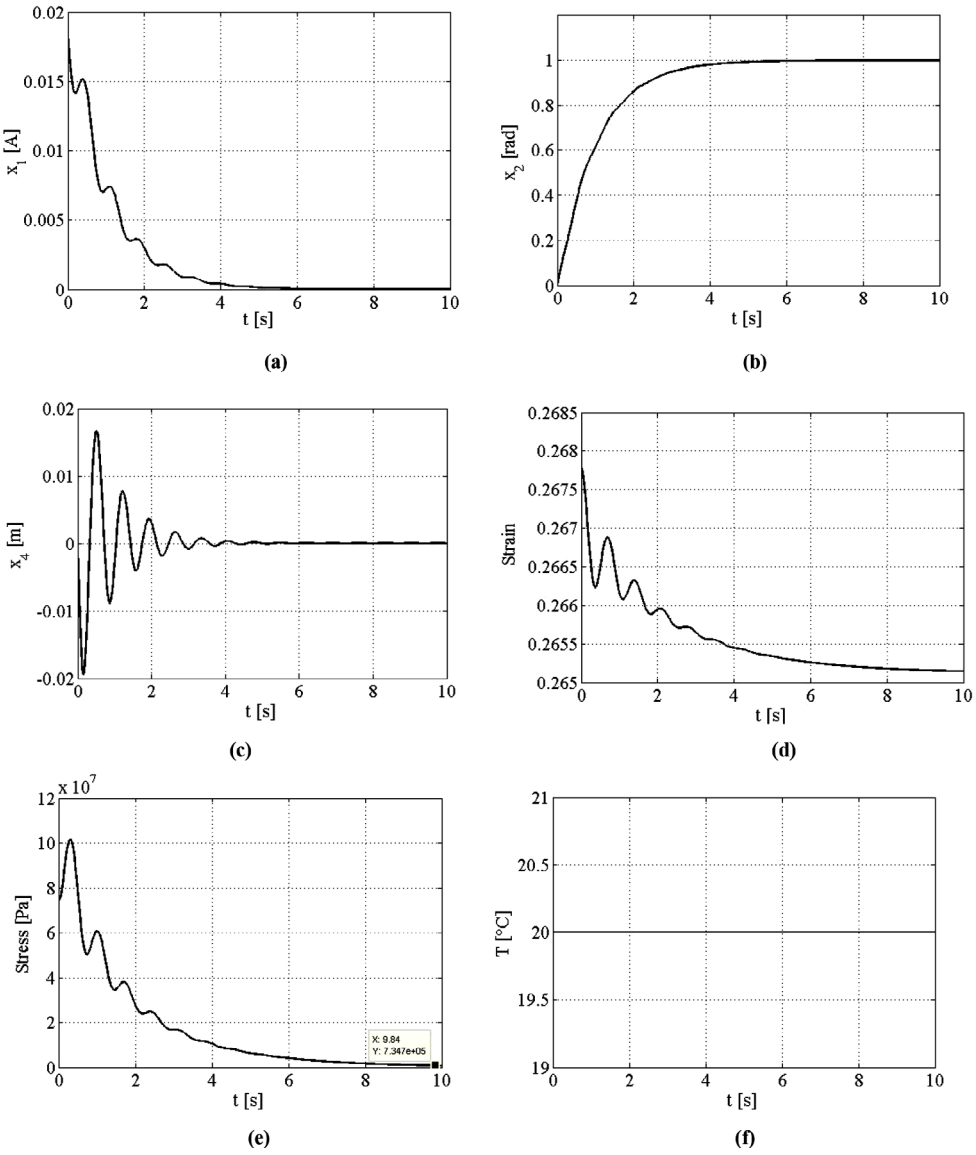

Fig. 2. Numerical simulation results for positioning control: (a) electric current applied to the DC motor terminals, (b) angular displacement of the beam and point, (c) vibration of the beam and point, (d) strain of the SMA actuator, (e) stress of the SMA actuator and (f) temperature of the SMA actuator.

Comparing Fig. 2(a) with Fig. 2(c), it is possible to observe the coupling of the beam like structure vibration to the DC motor shaft. By analyzing Fig. 2(a) which is the controlled variable of the positioning control, it can be seen that the SDRE control technique is acting to control the position of the beam, trying to correct the error caused by the beam vibration due to its flexibility. This can be confirmed looking at Fig. 2(b) which shows the angular displacement of the beam. The desired displacement of 1 radian was reached after 5.5 seconds. In this way, it is important to note that the positioning controller does not optimize the positioning time. Figure 2(d) presents

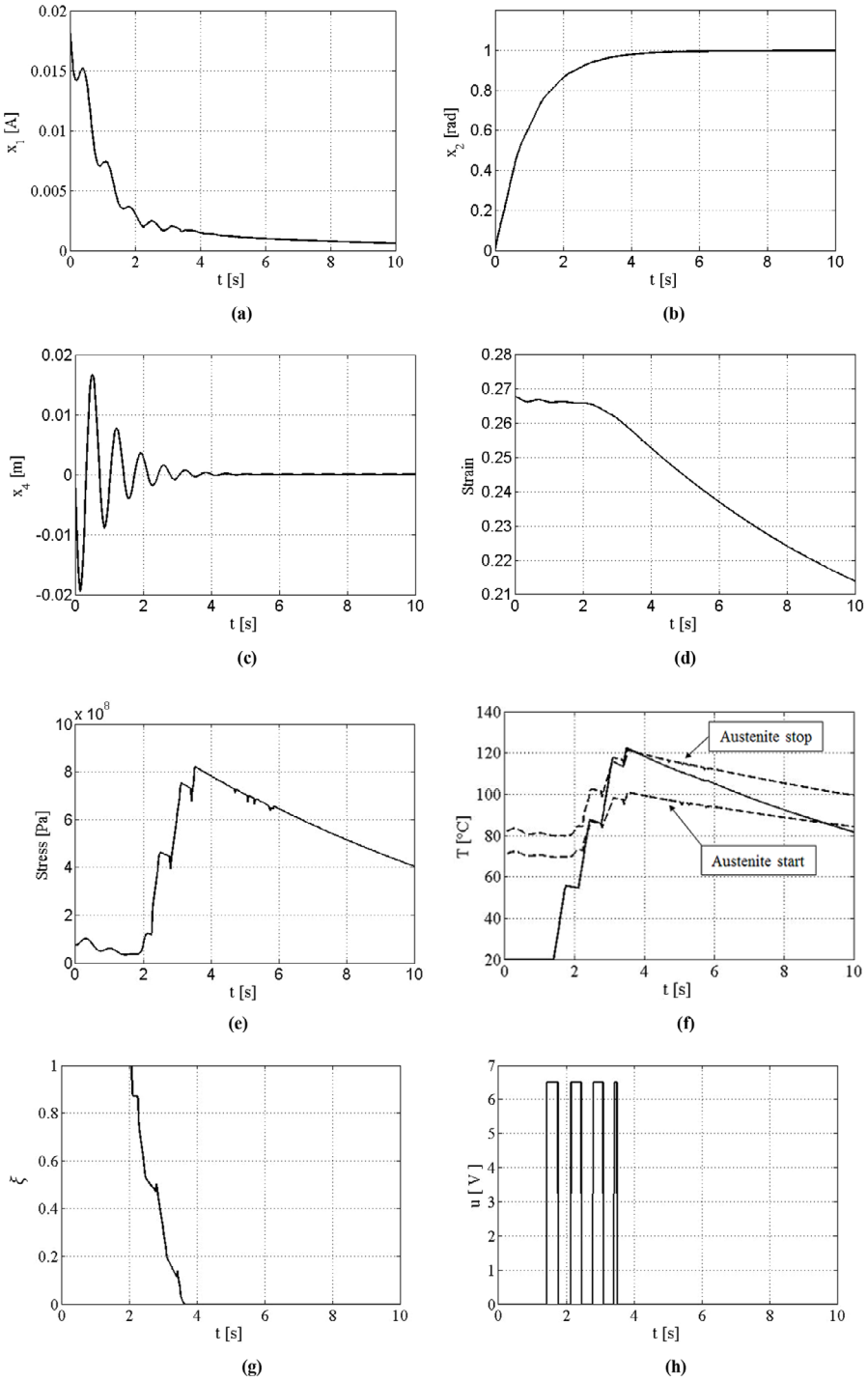

Fig. 3. Numerical simulation for position and vibration control: (a) electric current applied to the DC motor terminals, (b) angular displacement of the beam and point, (c) vibration of the beam and point, (d) strain of the SMA actuator, (e) stress of the SMA actuator, (f) temperature of the SMA actuator, (g) is the SMA phase transformation coefficient and (h) is the SMA actuator applied control signal u.

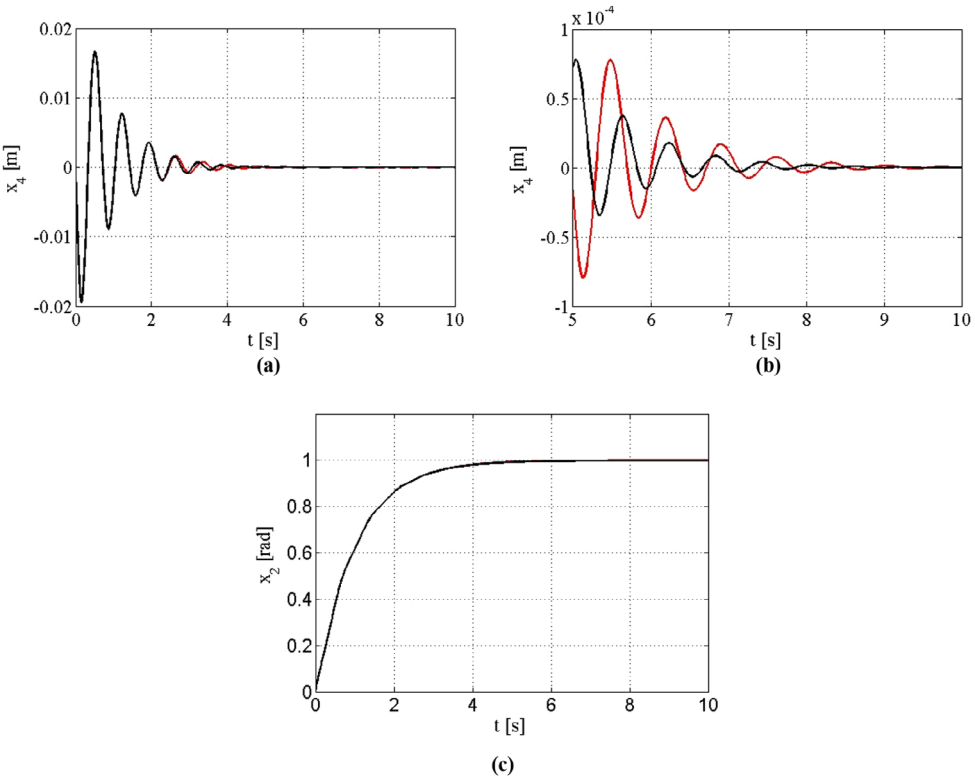

Fig. 4. Comparison between the control with and without the SMA actuation: (a) the black line is the vibration with the SMA control and the red line without the SMA control. (b) Zoom of the beam vibration settling time after the angular a positioning settling (c) the red line is the angular displacement with the SMA actuation and the black line is the angular displacement without the SMA control.

the strain variation of the SMA actuator due to the beam vibration. In the case when just the angular positioning of the beam is controlled, the temperature of the SMA remains the same, justifying Fig. 2(f), which does not present any variation on the SMA temperature.

Figure 3, displays results of numerical simulations of the case in which the angular positioning and the vibration of the flexible beam are controlled.

The stress increase in Fig. 3(e) is due to the phase transformation (martensite to austenite) and the decrease is explained by the phase change from austenite to martensite caused by the SMA temperature change. In Fig. 3(g) it is possible to see that the phase transformation of thTe SMA starts at 1.8 seconds and the complete phase transformation occurs at 3.6 seconds where the SMA stops the actuation.

Figure 3(h) presents the control signal applied to the SMA actuator, which has its saturation at 6.5 Volts.

Figure 4(a) presents a comparison between vibrations for the two control cases.

Figure 4(a) presents the comparison between the vibration of the beam with and without the SMA actuation. It is possible to see a phase shift in the natural frequency of the beam after 3 seconds, which is caused by the stiffness change due to the SMA actuation as shown in (Raghavan, et al. 2010). No difference is seen in Fig. 4(c) which presents the settling time of the of the angular positioning. In Fig. 4(b) it is possible

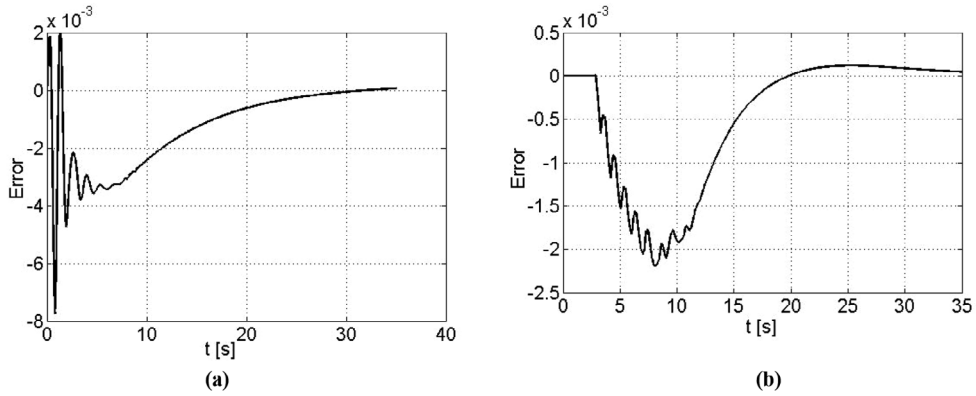

Fig. 5. Parametrical sensitivity of the positioning control, (b) parametrical sensitivity of the positioning and vibration control.

to see the vibration after the angular position reaches 1 radian. The result shows that the system with SMA actuation had a higher damping. Considering that the positioning of the system depends of the rigid body displacement and of the elastic displacement as showing in Eq. (1) it is possible to see in Fig. 4(b) that the system with the SMA actuation reaches the position about 0.8 seconds before the system without actuation.

5 Parametric sensitivity analisys

Parametric uncertainties are associated with discrepancies between the values of actual physical systems and the input parameters used in the analysis (Schueller, 2007; Triguero et al., 2013).

To consider the effects of parameter uncertainties on the performance of the controller, the parameters used in the control will be considered to have random error of ±20%, applied to the parameters of matrices A and B. Equations ((36)–(37)) and Eqs. ((41)–(42)). This strategy is similar to that used in (Balthazar et al., 2012; Nozaki et al., 2013; Tusset et al., 2013, 2015; Peruzzi et al., 2015).

Figures 5(a) and (b) show the parametric error analysis for both cases of control.

It is possible to see that the error of the system without vibration control is much larger than the with vibration control. But it is also possible to see that in the two cases the error leads to zero which is a good indicator of the robustness of the control technique applied in this work.

6 Conclusions

An active vibration and angular position control of a composite beam in slewing motion with a SMA actuator was presented.

Numerical results show that the application of the SDRE control was effective to control the angular position of a flexible beam (Fig. 2), and that the proposed control is robust to parametric errors (Fig. 5).

It was also possible to observe that with the vibration control, the beam spends less time to reach the desired point (Fig. 3). We can see that the vibration settling

time of the two cases (actuated and not actuated) is not large. But taking into consideration that the actuator is thin, relative to the beam, we can see that the result is positive. Taking into account that it is possible to increase the actuator thickness or use more than one actuator, it is possible to improve system performance, as shown in Yuvaraja and Senthilkumar (2012).

In Fig. 4 a change in the natural frequency of the beam can be seen, which is caused by the stiffness variation due to the SMA. This fact shows that it is possible to tune the natural frequency which makes it possible to take the beam out of a resonance region (Zhang et al. 2006).

The authors would like to acknowledge Conselho Nacional de Desenvolvimento Científico e Tecnológico – CNPQ (grant: 447539/2014-0) and (grant: 484729/2013-6).

References

1. J.M. Balthazar, D.G. Bassinello, A.M. Tusset, A.M. Bueno, B.R. Jr. Pontes (Milano Print) **1**, 1 (2014)
2. J.M. Balthazar, A.M. Tusset, S.L.T.D. Souza, A.M. Bueno, Proceedings of the Inst. Mech. Eng. Part C, J. Mech. Eng. Science **227**, 1730 (2012)
3. H.T. Banks, B.M. Lewis, H.T. Tram, Comput. Optim. Appl. **37**, 177 (2007)
4. L.C. Brinson, J. Intel. Mater. Systems Struct. **4**, 229 (1993)
5. M.H. Elahinia, H. Ashrafiuon, J. Vibration Acoustics **124**, 566 (2002)
6. M.H. Elahinia, T.M. Seigler, D.J. Leo, M. Ahmadian, J. Intel. Mater. Systems Struct. **15**, 495 (2004)
7. G. Ephrahim, Inman, D.J., Modeling of Actuator-Structure Interaction in the Slewing of Flexible Struct. American Control Conference 1962 (1990)
8. A. Fenili, J.M. Balthazar, R.M.L.R.F. Brasil, J. Sound Vibration **268**, 825 (2003)
9. A. Fenili, J.M. Balthazar, J. Sound Vibration **282**, 543 (2004)
10. F. Gantmacher, Lectures in Analytical Mech. Mir Publishers, Moscow (second printing) (1975)
11. E. Garcia, D.J. Inman J. Intel. Mater. System Struct. **261** (1991)
12. S.S. Ge, P.K. Tee, E.I. Vahhi, E.H.F. Tay, IEEE/ASME Transactions on Mechatronics **11**, 690 (2006)
13. K. Ikuta, IEEE Robotics and Automation Society, Los Alamitos, CA, IEEE Computer Soc. Press **3**, 2156 (1990)
14. F.C. Janzen, A.M. Tusset, V. Piccirillo, J.M. Balthazar, M. Silveira, B.R. Jr. Pontes, IMECE 2014- ASME 2014 Int. Mech. Eng. Congress & Exposition, 2014, Montreal, ASME **1** (2014)
15. J.J. Lima, A.M. Tusset, F.C. Janzen, V. Piccirillo, C.B. Nascimento, J.M. Balthazar, M.R. L.F. Brasil, J. **5**, 413 (2014)
16. L. Meirovitch, Analytical Methods in Vibrations (Macmillan Publishing, New York, 1967)
17. A. Molter, O.A.A. Silveira, Fonseca, S.O. Jun, V. Bottega, Math. Problems Eng. **1** (2010)
18. P.C. Mracek, J.R. Cloutier, Int. J. Robust Nonlinear Control **8**, 401 (1998)
19. N.J. Peruzzi, F.R. Chavarette, J.M. Balthazar, A.M. Tusset, A.L.P. Manfrim, R.M.L.R.D.F. Brasil, J. Vibration Control **1** (2015)
20. V. Piccirillo, J.M. Balthazar, B.R. Jr. Pontes, J.L. Palacios, Part I: ideal energy source, Nonlinear Dyn. **46**, 597 (2008)
21. J. Raghavan, T. Bartkiewicz, S. Boyko, M. Kupriyanov, N. Rajapakse, Yu, Ben.Composites: Part B **41**, 214 (2010)
22. D. Ramos, J. Mertens, M. Calleja, J. Tamayo, Sensors (Besel) **7**, 1757 (2007)
23. R. Romano, E.A. Tannuri, Mechatronics **19**, 1169 (2009)

24. G.I. Schueller, On the treatment of uncertainties in structural Mech. analysis. Comp. Struct. **85**, 235 (2007)
25. H. Sepiani, F. Ebrahimi, H. Karimipour, J. Mech. Science Tech. **23**, 3179 (2009)
26. M.O. Tokhi, A.K.M. Azad, Inst. Eng. Tech. (2008)
27. R.C. Triguero, S. Murugan, R. Gallego, M.I. Friswell, Mech. Systems Signal Processing **41**, 268 (2013)
28. A.M. Tusset, J.M. Balthazar, D.G. Bassinello, B.R. Pontes, J.L.P. Felix, Nonlinear Dyn. **69**, 1837 (2012a)
29. A.M. Tusset, J.M. Balthazar, J.L.P. Felix (2013b), J. Vibr. Control **803** (2012)
30. A.M. Tusset, A.M. Bueno, C.B. Nascimento, M.S. Kaster, J.M. Balthazar, Shock Vibration **20**, 749 (2013)
31. A.M. Tusset, V. Piccirillo, A.M. Bueno, J.M. Balthazar, D. Sado, J.L.P. Felix, R.M. L.R.D.F. Brasil, J. Vibration Control **1**, 1 (2015)
32. Z.G. Wei, R. Sandström, J. Mater. Science **33**, 3763 (1998)
33. M. Yuvaraja, M. Senthilkumar, J. Manuf. Ind. Eng. **11**, 28 (2012)
34. R. Zhang, Q. Ni, A. Masuda, T. Yamamura, M. Iwamoto, Composite Struct. **74**, 389 (2006)